Current Opinion in Solid State and Materials Science 16 (2012) 168–177

Contents lists available at SciVerse ScienceDirect

Current Opinion in Solid State and Materials Science

journal homepage: www.elsevier.com/locate/cossms

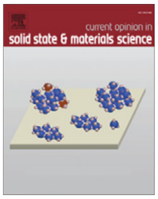

Sodium and sodium-ion energy storage batteries

Brian L. Ellis, Linda F. Nazar*

University of Waterloo, Department of Chemistry, Waterloo, Ontario, Canada N2L 3G1

A R T I C L E   I N F O

Article history:
Available online 26 April 2012

Keywords:
Energy storage
Sodium ion batteries
Sodium batteries
Solid state chemistry
Energy materials
Grid storage

A B S T R A C T

Owing to almost unmatched volumetric energy density, Li-ion batteries have dominated the portable electronics industry and solid state electrochemical literature for the past 20 years. Not only will that continue, but they are also now powering plug-in hybrid electric vehicles and electric vehicles. In light of possible concerns over rising lithium costs in the future, Na and Na-ion batteries have re-emerged as candidates for medium and large-scale stationary energy storage, especially as a result of heightened interest in renewable energy sources that provide intermittent power which needs to be load-levelled. The sodium-ion battery field presents many solid state materials design challenges, and rising to that call in the past couple of years, several reports of new sodium-ion technologies and electrode materials have surfaced. These range from high-temperature air electrodes to new layered oxides, polyanion-based materials, carbons and other insertion materials for sodium-ion batteries, many of which hold promise for future sodium-based energy storage applications. In this article, the challenges of current high-temperature sodium technologies including Na-S and Na-$NiCl_2$ and new molten sodium technology, Na-O_2 are summarized. Recent advancements in positive and negative electrode materials suitable for Na-ion and hybrid Na/Li-ion cells are reviewed, along with the prospects for future developments.

1. Introduction

Energy storage has become a growing global concern over the past decade as a result of increased energy demand, combined with drastic increases in the price of refined fossil fuels and the environmental consequences of their use. This has increased the call for environmentally responsible alternative sources for both energy generation and storage. Although wind and solar generated electricity is becoming increasingly popular in several industrialized countries, these sources provide intermittent energy; thus energy storage systems are required for load-leveling, i.e., storage of energy until needed by the electrical grid. Portable energy solutions that realize the practical use of hybrid electric vehicles (HEVs), plug-in hybrid electric vehicles (PHEVs) and purely electric vehicles (EVs) will further reduce dependence on fossil fuels.

Lithium-ion batteries, the most common type of secondary (rechargeable) cells found in almost all portable electronic devices, are a possible solution to these larger global concerns [1]. Lithium-based electrochemistry offers several appealing attributes: lithium is the lightest metallic element and has a very low redox potential ($E^{\circ}_{(Li^+/Li)} = -3.04$ V versus standard hydrogen electrode), which enables cells with high voltage and high energy density. Furthermore, Li^+ has a small ionic radius which is beneficial for diffusion in solids. Coupled with its long cycle life and rate capability, these properties have enabled Li-ion technology to capture the portable electronics market.

The demand for lithium-ion batteries as a major power source in portable electronic devices and vehicles is rapidly increasing: lithium-ion batteries are regarded as the battery of choice for powering future generations of HEV and PHEVs. With the likelihood of enormous demands on available global lithium resources, concerns over lithium supply – but mostly its cost – have arisen. Many global lithium reserves are located in remote or in politically sensitive areas [2,3]. Even if extensive battery recycling programs were established, it is possible that recycling could not prevent this resource depletion in time. Furthermore, increasing lithium utilization in medium-scale automotive batteries will ultimately push up the price of lithium compounds, thereby making large-scale storage prohibitively expensive.

With sodium's high abundance and low cost, and very suitable redox potential ($E^{\circ}_{(Na^+/Na)} = -2.71$ V versus standard hydrogen electrode; only 0.3 V above that of lithium), rechargeable electrochemical cells based on sodium also hold much promise for energy storage applications. The report of a high-temperature solid-state sodium ion conductor – sodium β″-alumina ($NaAl_{11}O_{17}$) – almost 50 years ago spawned tremendous interest both in the field of solid state ionics and sodium electrochemistry [4]. This material became the electrolyte/separator that was key to the development of two battery types that are commercially available: sodium sulfur (Na–S) and ZEBRA (Zero-Emission Battery Research Activities) cells

---

* Corresponding author.
E-mail address: lfnazar@uwaterloo.ca (L.F. Nazar).

1359-0286/$ - see front matter © 2012 Elsevier Ltd. All rights reserved.
http://dx.doi.org/10.1016/j.cossms.2012.04.002

which are based on Na-NiCl$_2$. Both cells operate at high temperature (near 300 °C) where sodium and the positive electrodes are molten (thus removing concerns over internal short circuits as a result of dendrite formation). The good ionic conductivity of the sodium β″-alumina membrane at the elevated temperatures further helps to lower cell impedance. Other fast sodium ion conductors have been under development in recent years, which have propelled this field forward, and led to the possibility of Na-batteries that operate at lower temperatures, i.e., either at room temperature or just above the melting point of sodium (100 °C). Sodium-*ion* cells based on intercalation materials that employ non-aqueous electrolytes, akin to lithium-ion batteries, were explored in the mid-1980s, and have undergone a renaissance in the last few years with quite a number of new materials and approaches having been reported.

After providing brief updates on new developments in Na–S and ZEBRA systems and a novel Na–O$_2$ battery design, we review the recent research highlights of sodium-ion based electrochemistry, with a focus on recent work on intercalation compounds for positive electrode materials for sodium intercalation (including layered transition metal oxides and polyanionic compounds) and negative electrodes (including hard carbons, titanium and vanadium oxides). The details of these technologies and some of the significant issues and opportunities provided by the field of sodium and sodium-ion batteries will be discussed herein.

2. Molten sodium cells (sodium batteries)

2.1. Sodium sulfur (Na–S) batteries

Sulfur, based on its low cost, high capacity, and environmental friendliness, has been heavily researched in the past as a positive electrode material. Typical Na-S cells contain molten sodium (the negative electrode) housed within a sodium β″-alumina tube which is surrounded by molten sulfur [5]. A schematic diagram of the high-temperature Na–S battery is shown in Fig. 1a. During discharge of the cell, sodium is oxidized and as the electrons pass through the external circuit, sodium ions pass through the β-alumina electrolyte to the positive electrode where they react with sulfur. The electrochemical profile is summarized in Fig. 1b. Initially, a two-phase region exists at 2.075 V between sulfur and the initial sodium polysulfide that is formed (Na$_2$S$_5$), as these two liquids are immiscible at the operating temperature [6]. Further reduction to Na$_2$S$_4$ occurs between 2.075 V and 1.74 V and proceeds *via* a solid-solution mechanism. Reduction to Na$_2$S$_3$ at 1.74 V occurs via a two-phase transition. At deeper discharge, a solid phase with a high melting point forms (Na$_2$S$_2$). At this point, increased resistance at the positive electrode prohibits further discharge, limiting the gravimetric capacity of the positive electrode to 836 mAh/g although full cells operate at much less than this.

Much research has been devoted to practical aspect of these cells, related to the high operation temperature (270–350 °C). At these temperatures, molten sulfur, sodium and the polysulfide compounds are highly corrosive: containers and seals must be resistant under these conditions. Chromized steel and molybdenum-lined steels have been shown to resist corrosion in these cells [7]. Since 2003, these cells – primarily manufactured by NGK, Japan – have been widely used for load-leveling and emergency power applications in 174 locations in six countries around the world, storing 305,000 kW of electricity. These have been incident free until September this year when a battery fire erupted at the Tsukaba Plant in Japan (although it was quickly brought under control without further ramifications).

Research on “low temperature” Na–S batteries, analogous to Li–S batteries which offer great promise as low-cost, high-capacity energy storage systems [8–10], is underway to mitigate some safety concerns. The cells operate either at room-temperature or just below 100 °C, and rely on conventional separators and organic electrolytes containing sodium salts such as NaPF$_6$; and a porous conductive carbon to contain the sulfur at the positive electrode. Unlike high-temperature Na–S cells, these cells have a much higher capacity: the theoretical gravimetric capacity of the sulfur electrode is 1672 mAh/g based on full reduction to Na$_2$S, although most reports fail to achieve a third of this capacity [11–13]. These low capacities are likely the result of the formation of soluble polysulfides which diffuse through the electrolyte to the negative electrode to form lower-order polysulfides. This phenomenon is also a common problem in Li-S cells, although it may be mitigated by coatings on the sulfur/carbon composite electrode [8]. The problem is exacerbated in the Na–S cell, however, owing to the much higher solubility of the polysulfide species. New approaches to devise protective layers for both the positive and negative electrode, and the development of improved electrolytes hold promise for the future of the “low”-temperature Na–S cell.

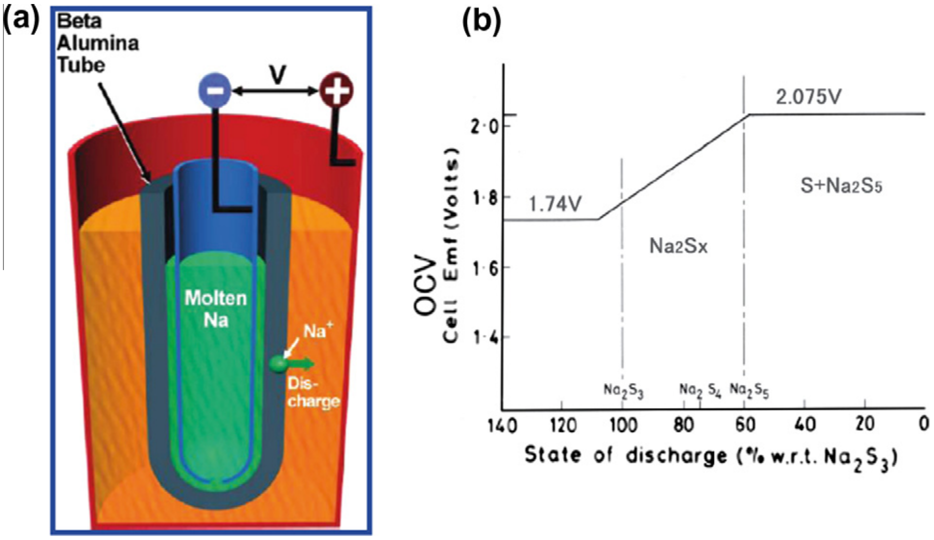

Fig. 1. (a) Schematic representation of the sodium sulfur cell, reproduced with permission from [101] and (b) representation of voltage profile for Na-S cell with phases present at each stage shown. Reproduced with permission from [6].

2.2. Sodium–air (Na–O_2) cells

Air electrodes operate by the reaction of oxygen with alkali metal ions to produce alkali oxides. The positive electrode employs porous carbon and/or porous metal as the current delivery system for O_2 reduction and as host for the product. The discharge reaction fills the voids with the oxide product and terminates when these voids are filled. Oxygen oxidation and reduction benefit from the use of a catalyst, usually dispersed on the porous matrix. Thus simultaneous contact is necessary for the reaction of alkali ions and oxygen molecules (present in the electrolyte) and electrons (delivered by the conductive matrix) for oxygen reduction at the catalyst sites on discharge. A representation of the Na–O_2 cell is shown in Fig. 2a. The potentials for reactions of sodium with oxygen are given below:

$$Na^+ + O_2 + e^- \rightarrow NaO_2 \quad E = 2.263\ \text{V} \tag{1}$$

$$2Na^+ + O_2 + 2e^- \rightarrow Na_2O_2 \quad E = 2.330\ \text{V} \tag{2}$$

$$4Na^+ + O_2 + 4e^- \rightarrow Na_2O \quad E = 1.946\ \text{V} \tag{3}$$

Although research on Li–O_2 batteries is fervent [14–19], Na–O_2 cells are in their infancy, with one on ambient temperature cells from Sun et al. [20] which followed the initial report on molten Na–O_2 cells from Peled et al. [21]. Sun's report proved to be interesting, however, the electrolyte used in the study was a mixture of organic carbonates and in Li–O_2 cells, carbonate-based electrolytes are known to decompose [22]. The oxide product formed on discharge in the Na–O_2 cell at ambient temperature was identified as Na_2O_2, possibly by decomposition of NaO_2. Under certain conditions, it may be possible to stabilize NaO_2.

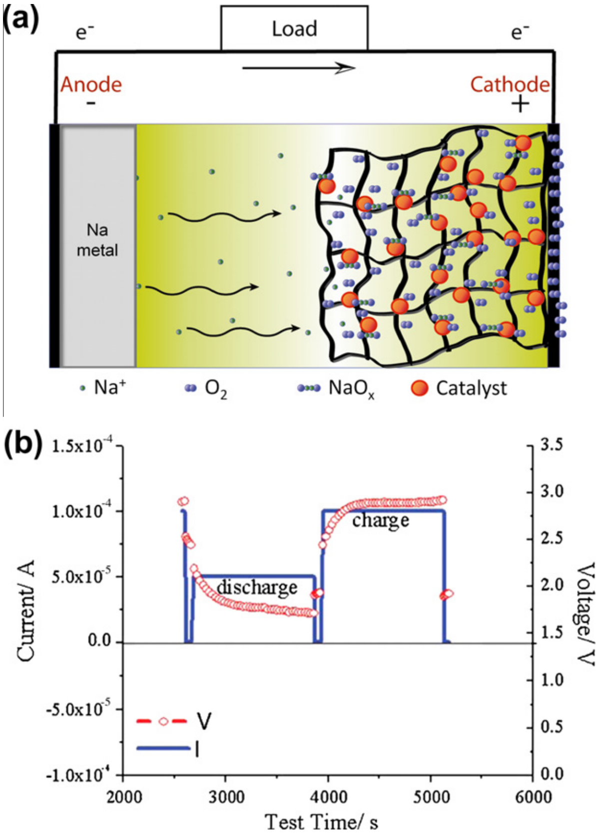

Fig. 2. (a) Schematic representation of Na-O_2 battery on discharge and (b) voltage profile for Na-O_2 battery on first discharge cycle. Reproduced with permission from [21].

Unlike Li–O_2 cells which normally operate at ambient temperatures, Peled replaced the metallic lithium anode with sodium and operated the cell above the melting point of sodium (98 °C) which prevented the formation of metallic dendrite formation on the negative electrode during charge. Additionally, at temperatures above 100 °C, the adsorption of water vapor by the cell components was negligible so minimal interference of atmospheric water was expected. The voltage profile of the high-temperature Na–O_2 cell using a polymer electrolyte is shown in Fig. 2b. The Na–O_2 cell exhibited a charging potential at 2.9 V and 1.8 V on discharge. With the discharge potential expected to lie around 2.3–2.4 V, the low discharge voltage suggests kinetic overpotential is a concern for this Na–O_2 cell, possibly due to the polymer electrolyte. In Li–O_2 cells, the overpotential is usually 0.3–0.4 V [23,24]. In addition, lithium metal reacts with the electrolyte to form a surface solid electrolyte interphase (SEI) layer, which is re-formed on continuous cycling [25]. Lithium dendrite formation on charge is thus a concern for Li–O_2 cells. The successful cyclability demonstrated in this initial Na–O_2 report will encourage the development of a new generation of high specific energy density rechargeable cells.

2.3. ZEBRA cells

ZEBRA cells were developed in the 1980s and contain a liquid sodium negative electrode and a metal chloride positive electrode, usually $NiCl_2$ [26]. More recent work has shown that addition of iron to the cell increases the power response [27–29]. The discharge reactions and potentials versus sodium at 300 °C are shown below:

$$NiCl_2 + 2Na \rightarrow Ni + 2NaCl \quad E = 2.58\ \text{V} \tag{4}$$

$$FeCl_2 + 2Na \rightarrow Fe + 2NaCl \quad E = 2.35\ \text{V} \tag{5}$$

A schematic of the sodium ion transport through the cell during discharge is shown in Fig. 3. Sodium ions which result from the oxidation of sodium at the negative electrode are transported through the solid sodium β″-alumina electrolyte to the $NiCl_2$ by a secondary electrolyte (a eutectic mixture of NaCl and $AlCl_3$). For most of the discharge, the system functions as a Na-$NiCl_2$ cell. If a high current pulse is applied to the cell and the working voltage falls below 2.35 V, the iron reaction augments the main nickel reaction: both discharge in parallel. This occurs at the front of the electrode and the cell therefore has its minimum resistance. When the working voltage recovers above 2.35 V, the iron produced is then reoxidized to $FeCl_2$ by the remaining nickel chloride and the $FeCl_2$ is then available for the next high current discharge.

An advantage of the ZEBRA cells is that they may be assembled in the discharged state with NaCl, Al, nickel and iron powder. Fur-

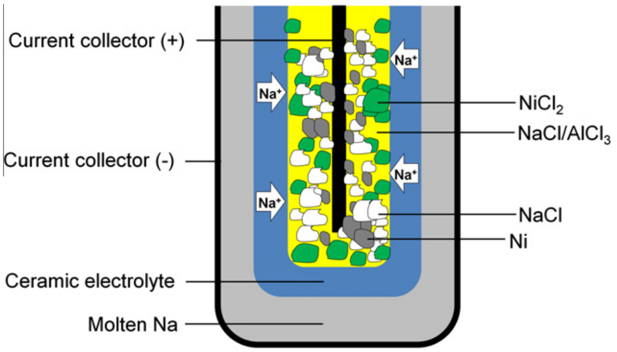

Fig. 3. Schematic representation of Na-$NiCl_2$ (ZEBRA) cell on discharge.

thermore, the positive electrode is comprised mostly of solid materials which reduces corrosivity and makes the cell intrinsically safer than the Na–S cell. Combined with the higher voltage, these cells may be of practical use in electric vehicles if the synthesis and processing of the sodium β″-alumina components are optimized, or if other better Na-ion solid state electrolytes are developed [30–32].

3. Sodium-ion batteries

Sodium batteries were initially researched alongside Li batteries in the late 1970s and through the 1980s [33–40] although the benefits of lithium batteries, namely higher energy density as a result of higher potential and lower mass, shifted the focus of the battery community away from sodium. Sodium-ion cells do not employ sodium as the negative electrode; they are comprised of hard carbons or intercalation compounds. The negative electrode is one of the most troublesome components of the sodium-ion cell, in fact, since typical graphitic carbons employed in Li-ion cells cannot be used as discussed below. On discharge, the negative electrode is oxidized and sodium is released into the electrolyte while the positive electrode intercalates sodium and undergoes reduction on discharge. A summary of potentials as well as theoretical and achieved capacities for positive and negative electrode materials for sodium-ion batteries is presented in Figure 4. Not surprisingly, many of the materials suitable for sodium-ion batteries are similar to those which have been exhaustively researched over the past 20 years for lithium-ion batteries, including layered transition metal oxides, olivines and compounds with the NASICON framework. Furthermore, sodium-containing positive electrode materials may be cycled with a sodium salt electrolyte in sodium-ion cells or versus lithium with a lithium salt electrolyte in hybrid Na/Li-ion cells as described for some of the compounds below.

3.1. Positive electrode materials for Na-ion batteries

3.1.1. Manganese oxides

$Na_{0.44}MnO_2$, first prepared *via* a solid-state route by Sauvage et al., has a structure comprised of wide tunnels which attracted attention as a possible positive electrode material for intercalation [41]. It offers the possibility of better cycling stability because of its ability to tolerate some stress during structural change. Insertion/deinsertion of sodium revealed capacities as high as 140 mAh/g over the course of multiple voltage steps (six biphasic transitions) within a potential range of 2–3.8 V. The insertion process within the Na_xMnO_2 system is fully reversible over the $0.25 < x < 0.65$ composition range although some irreversibility resulted when the material was charged beyond $Na_{0.25}MnO_2$. Single-crystal nanowires of the material display similar properties, with reversible capacity up to 128 mAh/g at a rate of C/10 and good capacity retention over 1000 cycles [42]. $Na_{0.44}MnO_2$ was also one of the first sodium-containing positive electrode materials cycled in a Li-ion cell to make a hybrid Li/Na-ion battery, using a polymer electrolyte ($PEO/LiCF_3SO_3$) [43]. The capacity for lithium in $Na_{0.44}MnO_2$ was similar to that of sodium: the full theoretical capacity (180 mAh/g) could also be reached in the case of lithium, albeit with notable capacity fade over 60 cycles. More recently, $Na_{0.44}MnO_2$ has been shown to cycle well in a sodium-ion polymer battery that employed a crystalline polymer system as the electrolyte, PEO_8NaAsF_6 [44]. And perhaps mostly importantly, the $Na_{0.44}MnO_2$ structure is also highly amenable to reversible Na de/insertion in *aqueous media*, where it has been studied in conjunction with an activated carbon negative electrode to create a water based Na-ion cell [45].

λ-MnO_2, prepared by chemical delithiation of the spinel $LiMn_2O_4$ is reported to become amorphous when cycled versus sodium although the disordered phase can intercalate up to 0.6 Na per formula unit between 2–4 V [46]. This material is also the subject of aqueous-based Na-ion battery systems that are under commercial development.

3.1.2. Layered oxides

Known for their commercial domination of the Li-ion battery market, layered oxides of the type AMO_2 (A = Li, Na; M = Co, Mn, Ni and combinations thereof) [47–50] are sought after for their high intercalation potentials and energy densities. The alkali cation A is reversibly de/intercalated between the two-dimensional layers of transition metal MO_6 octahedra on electrochemical cycling. Similar to the lithium metal oxides, sodium oxides can exist as one of several polytypes. They differ in the stacking of the oxygen layers (ABCABC for O3, ABBA for P2 and ABBCCA for P3, using the notation designated by Delmas), resulting in different intercalation sites for the alkali cation [51]. $LiMO_2$ materials with the “ideal” O3 layered structure (M = Co, Ni and mixtures with Mn) have been the most thoroughly studied owing to their excellent electrochemical characteristics;

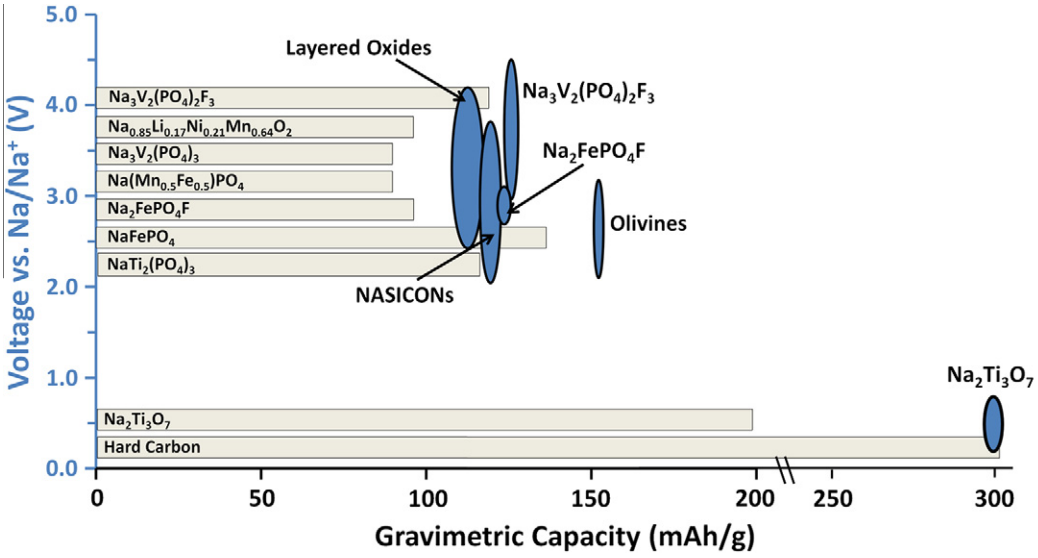

Fig. 4. Key positive and negative electrode intercalation materials for sodium-ion batteries: theoretical capacities of the various materials at their various potentials are shown with blue ovals, while achieved capacities are shown with gray bars. A detailed description of each group of compounds may be found in the text.

unfortunately Ti, Fe, or Mn do not crystallize in this phase as single metal compositions. Na_xMO_2 materials, in contrast, form the "ideal" ordered O3 – type layered structure more readily due to the larger ionic size difference between alkaline and transition metals that drives the segregation of the A and M into alternating layers. The deintercalation and intercalation of sodium in various layered Na_xMO_2 has been reported for a very wide variety of transition metals as briefly outlined in a recent report [52]. Of these, the manganese and cobalt oxides are the most viable for positive electrodes.

The known phases of Na_xMnO_2 ($x = 0.2, 0.40, 0.44, 0.70, 1$) include two for $x = 1$ [53]. The phase formed at lower temperatures, α-$NaMnO_2$, displays an O3 layered structure with a monoclinic structural distortion due to the Jahn–Teller distortion of the Mn^{3+} ion, whereas high temperature orthorhombic β-$NaMnO_2$ adopts a double stacked sheet structure. Computational studies indicate that the former is energetically more stable [54]. The electrochemical behavior of both α- and β-$NaMnO_2$ were reported by Mendiboure et al. in 1985, indicating that only 0.22 and 0.15 Na could be reversibly extracted and re-intercalated, respectively [55]. Recently, the electrochemical properties of the monoclinic α-$NaMnO_2$ have been revisited. In a significant improvement, the authors showed that about 0.8 Na can be reversibly de/intercalated with good capacity retention, corresponding to a 200 mAh/g capacity [49]. As the potential for Na de/insertion was the same, the reasons for the difference with the earlier work are not clear, although they may be related to the electrolyte. The previous report utilized $NaClO_4$ in propylene carbonate, whereas the latter used $NaPF_6$ in ethylene carbonate/dimethylcarbonate. The voltage profiles of monoclinic $NaMnO_2$ reveal very pronounced structural transitions on desodiation [49], which have also been observed in $NaCoO_2$; see below. These are much less common in Li intercalation oxides. They are likely due to Na-vacancy ordering or transitions that involve the gliding of oxygen planes, especially as Na likes to adopt both octahedral and trigonal prismatic environments and the latter can only be achieved in an O3 stacking by sliding some of the oxygen layers. The difference between the Li and Na oxides might be explained by the possibility that Na^+-vacancy ordering interactions are stronger due to sodium's larger cation radius. Alternatively, the oxygen layer gliding may be responsible, as it would allow optimization of Na coordination at each stoichiometry – which would not be as strong a driving force in the lithiated oxides. Overall, the effect is to create more cell hysteresis and reduce the energy efficiency somewhat. However, it is also interesting that 50% desodiation of $NaMnO_2$ does not result in conversion to a spinel as it does in the case of $Li_{0.5}MnO_2$ where migration of lithium to a tetrahedral site serves to trigger the transformation to spinel $LiMn_2O_4$. This ultimately results in capacity fading. This difference in behavior owes to the much higher relative stability of the Na^+ site in the intermediate layered $Na_{0.5}MnO_2$, that inhibits Na^+ migration. Good cyclability of the material results.

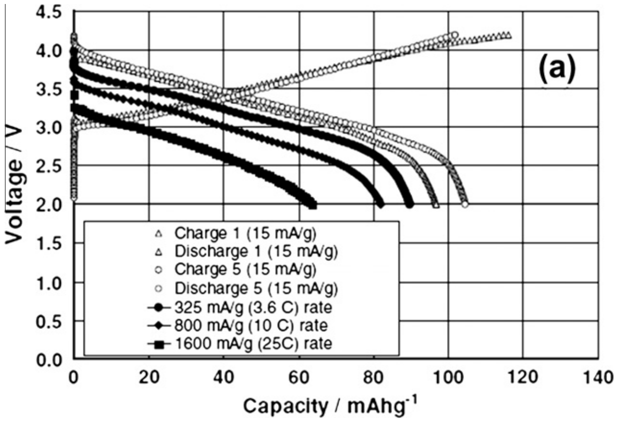

Fig. 6. Electrochemical potential of $Na_{0.85}Li_{0.17}Ni_{0.21}Mn_{0.64}O_2$ at various discharge rates. Reproduced with permission from [58].

Regarding cobalt oxides, Na_xCoO_2 exists as either the O3, P2 or P3 types, depending on the amount of Na intercalated. Of these, the P2 phase ($Na_{0.66}CoO_2$) is the most easily synthesized. The voltage profile (Fig. 5) shows that sodium extraction and reintercalation into $Na_{0.66}CoO_2$ occurs *via* several steps. Cells run at higher temperature (40 °C) retain the most stable electrochemical features (# 3, 8 and 9 from Fig. 5) and also maintain a similar capacity which indicates greater sodium mobility (disorder) and phase stability. Reduction of particle size of the synthesized compounds was found to improve electrochemical performance [56]. In contrast to the complicated mechanism of sodium extraction from the pure Co P2 phase, the P2 phase of $Na_{0.66}Co_{0.66}Mn_{0.33}O_2$ displayed solid-solution behavior on sodium extraction, except at the composition $Na_{0.50}Co_{0.66}Mn_{0.33}O_2$ where an ordered line-phase was found [57].

Another layered oxide, based on nickel(II)/manganese(IV) – $Na_{0.85}Li_{0.17}Ni_{0.21}Mn_{0.64}O_2$ – also displays promising electrochemistry [58] as shown in Fig. 6. Assuming the $Ni^{2+} \rightarrow Ni^{4+}$ redox reaction, the theoretical capacity is based on extraction of 0.42 Na (112 mAh/g). The voltage profile on discharge/charge was a smooth curve which

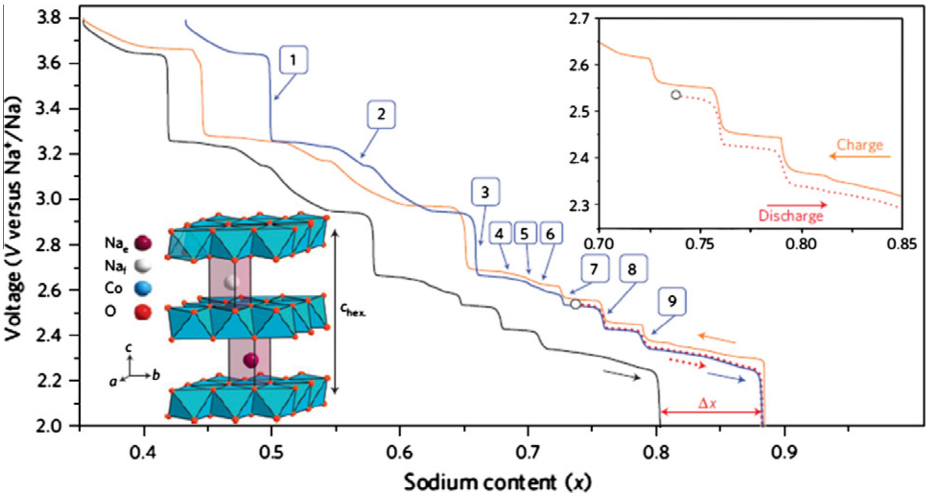

Fig. 5. Galvanic cycling of $Na_{0.7}CoO_2$, showing phase transitions on electrochemical cycling. Closeup of the region between $Na_{0.7}CoO_2$ and $Na_{0.85}CoO_2$ shown in right inset. Structure of $Na_{0.7}CoO_2$ shown in left inset. Reproduced with permission from [51].

indicated intercalation within a single phase. Impressive rate capability was demonstrated with this material: the observed discharge capacity of 65 mAh/g at high rate of 25 C (discharge in about 3 min) corresponds to a power density of about 670 W/kg.

The layered metal oxide structures are certainly amenable to sodium intercalation and extraction. A recent comprehensive article nicely contrasts the difference between Na and Li ion chemistries in a variety of compounds – including layered oxides, olivines and NASICONs – with respect to voltage, phase stability and activation energy for ion mobility [59]. The authors demonstrate that the generally lower calculated voltages for Na compounds are due to the smaller energy gain obtained from inserting Na into a host structure, versus that of Li. The differences, typically between 0.18 and 0.57 V, may be especially advantageous for the design of sodium battery negative electrode materials. Their calculations also show that Na^+ migration barriers may be lower than the corresponding Li^+ migration barriers in the layered structures. Although diffusional barriers are very structure dependent, this holds promise for the development of materials with improved kinetics.

3.1.3. NASICON-type materials

Compounds based on the 3-D structure of NASICON (NAtrium Super Ion CONductor) have been extensively studied for their structural stability and fast ion conduction, initially as solid electrolytes and more recently as insertion materials [60–62]. $NaNbFe(PO_4)_3$ and $Na_2TiFe(PO_4)_3$ were initially examined in 1992 by Tillement et al. [63] and the latter was also reported later by Masquelier and co-workers, along with $Na_2TiCr(PO_4)_3$ [64]. Iron-containing phosphate compounds are sought after as electrodes owing to their stability and environmentally benign character. The $Fe^{3+} \rightarrow Fe^{2+}$ redox potential in these compounds is quite low, around 2.4 V versus Na/Na^+ owing to the corner-shared framework which reduces the influence of the inductive effect [65]. Full reduction of Fe (to Fe^{2+}) and Ti (to Ti^{3+}) was observed on electrochemical cycling of $Na_2TiFe(PO_4)_3$ with a desirably small polarization. The intermediate voltage, however, makes them less attractive as positive electrodes, but not quite low enough to function as negative electrode insertion materials. Variations in composition to further lower the insertion potential are discussed later in the context of negative electrodes.

Sodium intercalation in $Na_3V_2(PO_4)_3$ was studied in 2002 by Yamaki et al. [66]. When placed initially in discharge, the capacity of this compound was found to be 50 mAh/g at 1.6 V versus Na. Furthermore, after the material was charged to the original stoichiometry, the material could be further charged at 3.4 V versus Na and the discharge capacity at this step was 90 mAh/g. As with other V^{3+} phosphates such as $LiVPO_4F$ [67], $Na_3V_2(PO_4)_3$ is an ideal candidate for fabrication of symmetric cells, owing to the range of oxidation states of vanadium. With that intent, it was revisited by the same group in 2010 [68], although cycling stability over several cycles was poor.

3.1.4. Olivines

The ability of the layered oxide structure and the 3D network of NASICON to flexibly accommodate ions in either their layered or large interstitial spaces allows the existence of stable versions of these compounds for both Na and Li. This is not the case with $LiFePO_4$ which crystallizes in the olivine structure [69]: the corresponding sodium compound, $NaFePO_4$, crystallizes in the maricite structure and is electrochemically inactive [70,71]. To evaluate the electrochemistry of the $FePO_4$ olivines versus sodium, the lithium analogue $LiFePO_4$ was prepared and the lithium was extracted to produce orthorhombic $FePO_4$ which was then cycled at a very slow rate (1 Li in 50 h) in a sodium cell. First reported in 2010 [72], the structure of the electrochemically intercalated $NaFePO_4$ confirmed that this compound retained the olivine framework with a unit cell volume of 320.14 Å^3. It exhibits a volume contraction on Na extraction of almost 15%, more than twice that of Li–olivine (6.7%). Such large volume changes on de/insertion are common for Na-polyanion materials owing to the larger size of the Na^+ cation versus Li^+, and can result in slow kinetics due to the higher energy needed to move the phase boundary in two-phase reactions. The electrochemical curve is shown in Fig. 7a. On initial discharge, a voltage plateau at 2.8 V versus Na/Na^+ was observed and maintained until full insertion. On charge, a plateau indicative of a two-phase transition was observed at 3.0 V. Formation of a new single phase ordered line-phase at the composition $\sim Na_{0.7}FePO_4$ is signalled by a shift of the plateau up to 3.2 V. The structure has not yet been identified, and subsequent cycling showed quick capacity fade [71]. The potentials observed for electrochemical cycling are in good agreement with those predicted by calculations [73]. Amorphous $FePO_4$ prepared at 100 °C was also found to intercalate sodium with a reversible capacity of 100 mAh/g [74].

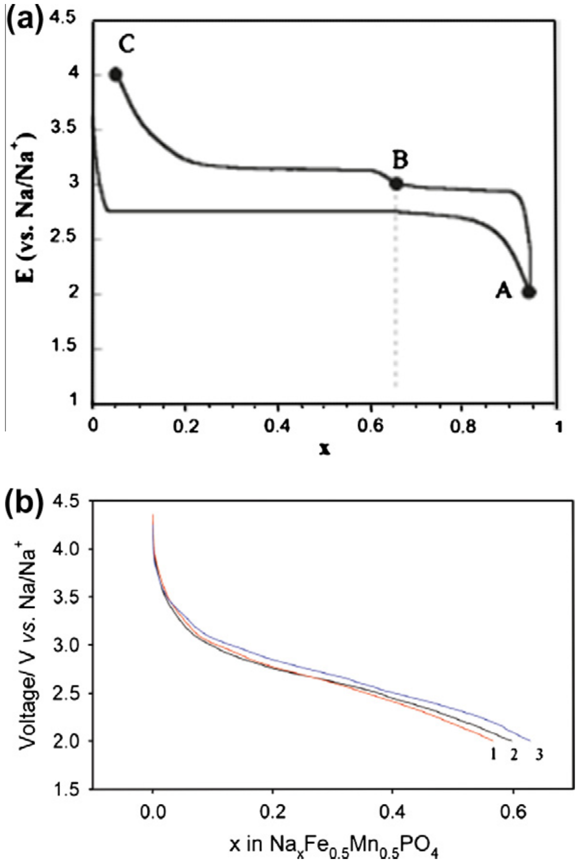

Fig. 7. (a) Electrochemical profile of olivine-$FePO_4$ intercalated with sodium. Reproduced with permission from [72] and (b) electrochemical profile of $Na(Fe_{0.5}Mn_{0.5})FePO_4$ cycled in a sodium cell. Reproduced with permission from [75].

Unlike the pure iron olivine, sodium iron/manganese olivine phosphate, $Na(Fe_{0.5}Mn_{0.5})PO_4$, could be synthesized directly *via* a molten salt reaction [75]. The electrochemical profile is shown in Fig. 7b. Interestingly, the electrochemical profile of $Na(Fe_{0.5}Mn_{0.5})PO_4$ exhibited a sloping profile over the entire voltage range when cycled versus sodium, with a somewhat low average potential of 2.7 V suggestive of a kinetic limitation. The origin of this solid solution behavior, confirmed by XRD measurements, is still under investigation, although it could be the result of transition metal cation (Fe^{3+}/Mn^{2+}) disorder as observed previously for $Li_x(Mn_yFe_{1-y}PO_4$ ($0 \leqslant x, y \leqslant 1$) [76].

3.1.5. Sodium vanadium fluorophosphates

The high potential of the $V^{3+} \rightarrow V^{4+}$ redox transition raises the cell voltage of these polyanionic materials compared to those described above. Two vanadium fluorophosphates based on this transition have been reported to date: $NaVPO_4F$ and $Na_3V_2(PO_4)_2F_3$. Studies on $NaVPO_4F$ demonstrated that Na extraction occurs over two different voltage plateaus in a sodium-ion cell: one at 3.0 V and the other at 3.7 V, indicative of a structural transformation [77]. Furthermore, Sauvage et al. [78] produced a new compound, $Na_3(VO)_2(PO_4)_2F$, from the same precursors used to make "$NaVPO_4F$" which caused the authors to call the stoichiometry of Barker's material into question. This new vandyl compound exhibited a reversible capacity of 87 mAh/g over the course of two different voltage plateaus at 3.6 V and 4.0 V versus Na.

$Na_3V_2(PO_4)_2F_3$ was cycled in a unique hybrid Na/Li-ion cell with graphite as the negative electrode and a lithium salt electrolyte [79]. Cycling data collected at charge/discharge rates of C/2 and 2C showed an initial cathode reversible capacity of 115–120 mAh/g, and the cells cycled with little capacity fade behavior after 400 cycles. Na/Li ion exchange was thought to occur in solution, thus the Li ions, and not the Na ions, intercalated into the graphite. This was the objective, since Na intercalation into graphite is not reversible. These data demonstrate the stability of this novel battery configuration where a sodium-containing positive electrode material may be paired with a Li electrolyte and graphite to achieve electrochemical reactivity.

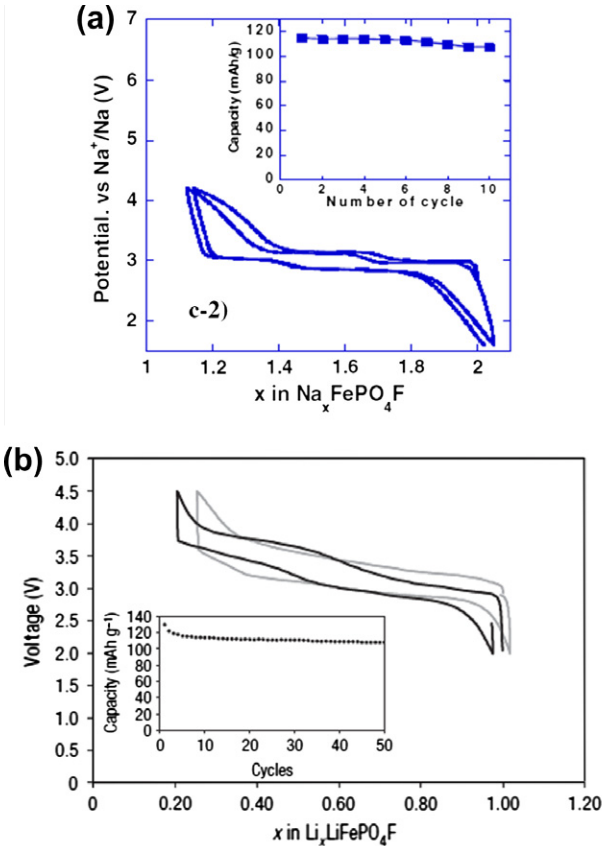

Fig. 8. (a) Electrochemical profile of Na_2FePO_4F cycled versus sodium at a rate of C/15. Reproduced with permission from [82] and (b) electrochemical profile of Na_2FePO_4F cycled in a lithium cell showing the first cycle (grey) and the second cycle (black) at a rate of C/10. Reproduced with permission from [70].

3.1.6. Layered sodium iron fluorophosphate

Na_2FePO_4F was first reported by our group in 2007 and was found to be isostructural with the previously reported Mg [80] and Co [81] sodium fluorophosphates which adopt a layered structure. Two-dimensional iron phosphate sheets house two Na^+ cations: Na (1) sits exactly between the layers and the Na (2) resides close to the phosphate sheets. The layered structure of Na_2FePO_4F allows for minimal structural modification on sodium deintercalation. The volume change between Na_2FePO_4F and $NaFePO_4F$ on extraction of Na (2) is 3.7% [70], much lower than that found for the sodium olivine (~15%) [59]. This results from the highly beneficial effect of the Na (1) ion. It cannot be electrochemically removed by oxidation owing to the inaccessibly high potential of the $Fe^{3+/4+}$ couple, and remains as a "pillar" between the layers to prop them apart. The kinetics of transport are also enhanced as the layers do not collapse. The material was also prepared by Armand et al., using a novel ionothermal synthesis route (solution phase synthesis in an ionic liquid) that afforded good crystallinity. The electrochemical profile of Na_2FePO_4F cycled versus sodium is shown in Fig. 8a. Both charge and discharge profiles appear to contain two two-phase plateaus, centered at 2.90 V and 3.05 V versus Na/Na^+, and 80% of the 120 mAh/g theoretical capacity was sustained on cycling [82]. A shift in the electrochemical potential observed halfway through the charge and discharge cycles is in good agreement with a structural distortion observed for the single phase compound, $Na_{1.5}FePO_4F$ observed previously [65].

When cycled versus Li/Li^+, Na_2FePO_4F demonstrated very different electrochemical properties. Representative electrochemical profiles for these cells are shown in Fig. 8b. Even before charging the cell, evidence of Li/Na ion exchange in the positive electrode was found [83]. The voltage profile for the first cycle resembles that found for the sodium cells but no flat two-phase regions were observed, which indicated Na/Li disorder in the positive electrode induced solid-solution like behavior [70]. The average voltage was about 3.4 V versus Li/Li^+ and the capacity was very stable over 50 cycles. Further ion exchange occurred on subsequent cycles such that the electrochemical profile continued to evolve: note the differences between the first and second cycles in Fig. 8b. The electrode material eventually reached a stable composition of $Li_{1.5}Na_{0.5}FePO_4F$ after about 20 cycles, suggesting that this is the limiting case for ready Na/Li exchange [83].

3.1.7. Tavorite sodium iron fluorosulfate

Nano-crystalline $NaFeSO_4F$ was prepared by a topotactic solvothermal reaction of $FeSO_4 \cdot H_2O$ and NaF in glycol [84] or ionic liquids [85]. The structure of $NaFeSO_4F$ is similar to that of the natural mineral tavorite ($LiFePO_4OH$) [86]. It is comprised of a corner-shared $FeSO_4F$ framework with sodium ions residing in spacious tunnels that run along the [1 1 0] direction. Atomistic modelling studies were performed to determine the activation energy of Na-hopping in this material. They revealed that sodium ion hopping between the tunnels (in the [1 0 1] direction) has a lower activation energy (0.6 eV) than in other directions where values as high as 1 eV dominate, and thus $NaFeSO_4F$ is effectively a 1-D ion conductor [87]. This is in sharp contrast to $LiFeSO_4F$ which exhibits activation energies for Li^+ ion hopping in multiple crystallographic directions between 0.35 and 0.44 eV as a consequence of its slightly different (albeit fairly similar) structure. The limited ion mobility of the Na analogue, along with a large volume change on redox, adversely affects the electrochemistry: $NaFeSO_4F$ displayed minimal reversible extraction of sodium, as less than 10% could be removed from the structure [84,85]. This illustrates the difficulty of extending solid state electrochemistry concepts from a lithium to a sodium analogue even when they are almost isostructural.

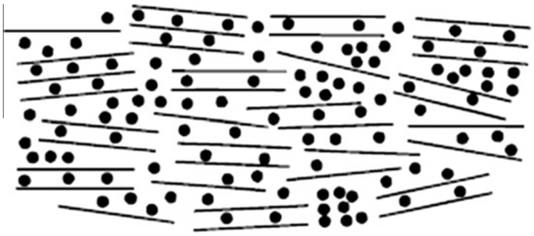

Fig. 9. Representation of the manner of which sodium intercalates into hard carbon, the "house of cards" model. Reproduced with permission from [92].

3.2. Negative electrode materials for Na-ion batteries

3.2.1. Carbon materials

Graphite, the common negative electrode in Li-ion batteries, cannot be used as an insertion electrode in Na-ion batteries as Na atoms do not intercalate between the carbon sheets [88–90]. Other carbonaceous materials have been investigated, however, and show promise. Sodium intercalation was observed in petroleum cokes,[91] along with hydrogen-containing carbon, soft carbons (small regions of ordered graphene) and hard (disordered) carbons [90,92]. The potential of Na insertion into hard carbon is close to that of the metal itself, which indicates there was very little carbon to sodium charge transfer. This would occur if the sodium inserted into the carbon *via* pores at the surface. Sodium was found to intercalate between the disordered layers of the hard carbon, as shown in the schematic diagram in Fig. 9. Hard carbon prepared from glucose demonstrated a capacity of 300 mAh/g at a slow intercalaction rate (C/80).

More recently, a non-graphitic carbon based on a porous silica template was prepared by Wenzel et al. in 2011 [93]. The high porosity enhanced the electrochemical performance at higher rates: a capacity of 180 mAh/g was achieved on the first cycle at a rate of C/5, but faded to 80 mAh/g after 125 cycles. This carbon outperformed several other industrial carbons, though, likely as a result of the carbon microstructure and porosity.

3.2.2. Low potential metal phosphates

Sodium insertion into the NASICON-type $NaTi_2(PO_4)_3$ for both aqueous and non-aqueous cells was reported by Park et al. in 2011 [94]. Na intercalates into this compound by a two-phase mechanism at 2.1 V versus Na/Na^+. The observed capacities for $NaTi_2(PO_4)_3$ in non-aqueous and aqueous electrolytes on cycling were 120 and 123 mAh/g respectively, which corresponds to over 90% of the theoretical capacity of 133 mAh/g. The polarization observed in the aqueous electrolyte on cycling was substantially smaller than in non-aqueous electrolyte, especially at a large current density, as a result of the lower impedance and the viscosity of the aqueous electrolyte. The Na-ion insertion/extraction potential is located at the lower limit of the electrochemical stability window of the aqueous Na_2SO_4 electrolyte, which makes $NaTi_2(PO_4)_3$ an attractive negative electrode for aqueous sodium-ion batteries.

3.2.3. Low potential sodium metal oxides

An interesting report on sodium intercalation into amorphous TiO_2 nanotubes was presented in 2011 [95]. No significant intercalation of sodium ions was observed when narrow TiO_2 nanotubes (<45 nm inner diameter, 10 nm wall thickness) were cycled versus sodium. However, as the size of the nanotubes were increased to >80 nm inner diameter, wall thickness >15 nm, Na intercalation *was* observed: cells cycled at a rate of C/3 exhibited a capacity of 100 mAh/g between 2.5 and 0.9 V versus Na/Na^+ on the first cycle, which increased gradually on cycling to reach 140 mAh/g on the 15th cycle. The improved intercalation properties for the larger tubes was attributed to the fact that they should have a greater number of Na^+ charge carriers (because of the greater volume of electrolyte contained within the tube) and hence could more easily establish a critical ion concentration.

A recent report on layered $Na_2Ti_3O_7$ suggests it has the lowest potential of any Na intercalation compound thus far [96]. Reduction takes place with the observation of a reversible plateau around 0.3 V versus Na/Na^+ (Fig. 8), which is quite remarkable. At this potential, two additional sodium ions were intercalated into the structure at a C/25 rate which corresponds to a capacity of 200 mAh/g and reduction of 2/3 of the Ti^{4+} to Ti^{3+}.

Vanadium oxides are also known to exhibit low potential alkali intercalation chemistry. Sodium deinsertion from the O3 phase of $NaVO_2$ has been examined by Delmas et al. in a detailed study that elucidated many of the complex structural changes that take place [97]. On deintercalation, the phase adopts a monoclinic distortion to form an O′3 structure where the octahedral site occupation of Na^+ is preserved (it is interesting to note that in contrast, chemical oxidation of $NaVO_2$ induces a switch from octahedral to prismatic coordination of the Na^+ cation [98]). Electrochemical deintercalation is reversible up to at least 0.5 mol Na per mole, corresponding to a capacity of 126 mAh/g of active material. Single line-phases were identified for both $Na_{1/2}VO_2$ and $Na_{2/3}VO_2$ compositions. Similar studies were later reported by Hamani et al. who confirmed the existence of these phases [99]. The voltage profile of each compound goes through several steps on both oxidation and reduction between 1.2 V and 2.4 V, although above 2.4 V an electrochemically inactive phase formed. While both compounds exhibit good reversibility on initial cycling, $Na_{0.7}VO_2$ displays very low polarization, a possible indicator of good performance at high rates. Nonetheless, the large voltage variation during cycling and the extreme oxygen sensitivity of $NaVO_2$ present challenges for practical applications.

Another vanadium oxide with a tunnel structure, NaV_6O_{13}, was prepared in nanorod morphology *via* hydrothermal synthesis [100]. The electrochemical profile contained two distinct plateaus at 2.7 V and 2.3 V before the main plateau at 1.7 V versus Na/Na^+, making it a slightly high voltage negative electrode material. It is also prone to substantial capacity loss at low cycling rates.

3.2.4. Alloys

As recently noted by Ceder [73], little research has been done thus far on sodium alloy materials as negative electrodes for sodium-ion batteries, although silicon alloys are well-researched for Li-ion batteries. The electrochemical sodiation of lead has been reported and up to 3.75 Na per Pb were found to react [39]. The same fraction of sodium might be expected to react with Sn, as $Na_{15}Sn_4$ is a known compound, although Si and Ge might be expected to uptake less sodium: the only known alloys of sodium/silicon and sodium/germanium are NaSi and NaGe. Nevertheless, since full lithiation of silicon alloys is not typically sustained in any case in order to avoid large volume changes, this may not present a problem. The potentials for these reactions were recently predicted [73], and show promise for future explorations.

4. Conclusions

Owing to concerns over lithium cost and sustainability of resources, sodium and sodium-ion batteries have re-emerged as promising candidates for both portable and stationary energy storage. Molten Na cells based on Na–S and Na–$NiCl_2$ developed in the last decade are commercially available and are especially of use for large-scale grid-applications; but new directions include "lower temperature" (i.e., 100 °C) Na–S and Na–O_2 cells, as well as ambient temperature Na–O_2 cells. These initial reports on Na–O_2

technology provide intriguing possibility with very high capacities as well as relatively low polarization.

In terms of ambient-temperature cells that operate on the basis of intercalation chemistry, many positive electrode materials reported thus far have been analogues of various Li-battery materials such as the layered oxides, NASICON compounds and olivines. Typically, the sodium and lithium compounds are not strictly isostructural though, especially in the case of polyanion materials where the influence of the alkali size/charge ratio is significant in determining the thermodynamically most stable phase. Thus, different electrochemical properties result and intriguing differences have emerged between the Li^+ and Na^+ cation systems. Similar observations are true for negative electrode materials: hard carbons, but not the graphitic materials that are used in Li-ion cells, have been reported to be active Na-ion intercalation compounds at low potential. Much scope for porous carbon design lies in this area. Sodium metal dioxides based on vanadium and titanium have also been studied for their low voltage properties. Intriguingly, modelling studies have revealed that the activation energy for Na^+-ion hopping is often lower than for Li^+ (perhaps due to less polarization), especially for layered oxides. The generally lower voltage of Na compounds also provides considerable advantages for negative electrode development by increasing the overall voltage and hence energy density. Of course, the potential of the sodium-containing positive electrode would be similarly lowered, but here there is the opportunity to explore materials where the lithium analogues have too high a potential to support many conventional electrolytes.

Based on electrochemical studies – not surprisingly – open and layered structures which are better able to accommodate the large Na^+ ions have proven to hold the most promise of the intercalation compounds. In terms of phase stability, these structures also generally have exhibit Na and Li versions of the same compound. However, as illustrated by Na_2FePO_4F, the development of new structures and framework types based specifically on sodium (i.e., not variations on the lithium analogue) are more likely to be pivotal for advancement of the Na-ion battery field. For intercalation systems, this means overcoming the larger volume expansion/contraction afforded by the sodium cation with clever solid state structure design. Overall, though, it is clear that Na-ion batteries can vie with Li-ion batteries in several important respects, and there is furthermore much opportunity and promise in this area.

Acknowledgments

NSERC is acknowledged for financial assistance through the Discovery Grant Program and for generous support *via* a Canada Research Chair to LFN. We are especially grateful to General Motors and NSERC for funding through the Collaborative Research Program.

References

[1] Tarascon JM, Armand M. Issues and challenges facing rechargeable lithium batteries. Nature 2001;414:359.
[2] Risacher F, Fritz B. Origin of salts and brine evolution of Bolivian and Chilean Salars. Aquat Geochem 2009;15:123.
[3] Yaksic A, Tilton JE. Using the cumulative availability curve to assess the threat of mineral depletion: the case of lithium. Resour Policy 2009;34:185.
[4] Fang Y, Yao Y, Kummer JT. Ion exchange properties of and rates of ionic diffusion beta alumina. J Inorg Nucl Chem 1967;29:2453.
[5] J.T. Kummer, N. Weber, Battery Having a Molten Alkali Metal Anode and Molten Sulfur Cathode, US Patent US 3413150, 1968.
[6] Oshima T, Kajita M. Development of sodium–sulfur batteries. Int J Appl Ceram Technol 2004;1:269.
[7] Dunn B, Breiter MW, Park DS. In situ evaluation of container corrosion in sodium–sulphur batteries. J Appl Electrochem 1981;11:103.
[8] Ji X, Lee KT, Nazar LF. A highly ordered nanostructured carbon–sulphur cathode for lithium–sulphur batteries. Nat Mater 2009;8:500.
[9] Ji X, Black R, Linda F. Stabilizing lithium–sulphur cathodes using polysulphide reservoirs. Nat Commun 2011;2:325-1.
[10] He G, Ji X, Nazar L. High “C” rate Li–S cathodes: sulfur imbibed bimodal porous carbons. Energy Environ Sci 2011;4:2878.
[11] Wang J, Yang J, Nuli Y, Holze R. Room temperature Na/S batteries with sulfur composite cathode materials. Electrochem Commun 2007;9:31.
[12] Park C-W, Ryu H-S, Kim K-W, Ahn J-H, Lee J-Y, Ahn H-J. Discharge properties of all-solid sodium–sulfur battery using poly (ethylene oxide) electrolyte. J Power Sources 2007;165:450.
[13] Ryu H, Kim T, Kim K, Ahn J-H, Nam T, Wang G, et al. Discharge reaction mechanism of room-temperature sodium–sulfur battery with tetra ethylene glycol dimethyl ether liquid electrolyte. J Power Sources 2011;196:5186.
[14] Hassoun J, Croce F, Armand M, Scrosati B. Investigation of the O_2 electrochemistry in a polymer electrolyte solid-state cell. Angew Chem Int Ed 2011;50:2999.
[15] Oh SH, Yim T, Pomerantseva E, Nazar LF. Decomposition reaction of lithium bis(oxalato)borate in the rechargeable lithium–oxygen cell. Electrochem Solid-State Lett 2011;14:A185.
[16] Ogasawara T, Debart A, Holzapfel M, Novak P, Bruce PG. Rechargeable Li_2O_2 electrode for lithium batteries. J Am Chem Soc 2006;128:1390.
[17] Kraytsberg A, Ein-eli Y. Review on Li–air batteries – opportunities, limitations and perspective. J Power Sources 2011;196:886.
[18] Ren X, Zhang SS, Tran DT, Read J. Oxygen reduction reaction catalyst on lithium/air battery discharge performance. J Mater Chem 2011;21:10118.
[19] Abraham KM, Jiang Z. A polymer electrolyte-based rechargeable lithium/oxygen battery. J Electrochem Soc 1996;143:1.
[20] Sun Q, Yang Y, Fu Z-W. Electrochemical properties of room temperature sodium–air batteries with non-aqueous electrolyte. Electrochem Commun 2012;16:22.
[21] Peled E, Golodnitsky D, Mazor H, Goor M, Avshalomov S. Parameter analysis of a practical lithium– and sodium–air electric vehicle battery. J Power Sources 2011;196:6835.
[22] Freunberger SA, Chen Y, Peng Z, Griffin JM, Hardwick LJ, Bardé F, et al. Reactions in the rechargeable lithium–O_2 battery with alkyl carbonate electrolytes. J Am Chem Soc 2011;133:8040.
[23] Lu Y-C, Kwabi DG, Yao KPC, Harding JR, Zhou J, Shao-horn Y. The discharge rate capability of rechargeable Li–O2 batteries. Energy Environ Sci 2011;4:2999.
[24] Lu Y-C, Xu Z, Gasteiger HA, Chen S, Hamad-schifferli K. Platinum–gold nanoparticles: a highly active bifunctional electrocatalyst for rechargeable lithium–air batteries. J Am Chem Soc 2010;132:12170.
[25] Bruce PG, Hardwick LJ, Abraham KM. Lithium–air and lithium–sulfur batteries. MRS Bull 2011;36:506.
[26] Sudworth JL. The sodium/nickel chloride (ZEBRA) battery. J Power Sources 2001;100:149.
[27] Bohm H, Beyermann G. ZEBRA batteries, enhanced power by doping. J Power Sources 1999;84:270.
[28] Galloway RC, Haslam S. The ZEBRA electric vehicle battery: power and energy improvements. J Power Sources 1999;80:164.
[29] Javadi T, Petric A. Thermodynamic analysis of reaction products observed in ZEBRA cell cathodes. J Electrochem Soc 2011;158:700.
[30] Sullivan TMO, Bingham CM, Clark RE. Zebra battery technologies for the all electric smart car. In: International symposium on power electronics, electric drives, automation and motion; 2006. p. S34–6.
[31] van Zyl A. Review of the zebra battery system development. Solid State Ionics 1996;86–88:883.
[32] Brett DJL, Aguiar P, Brandon NP. System modelling and integration of an intermediate temperature solid oxide fuel cell and ZEBRA battery for automotive applications. J Power Sources 2006;163:514.
[33] Whittingham MS. Chemistry of intercalaction compounds: metal guests in chalcogenide hosts. Prog Solid State Chem 1978;12:41.
[34] Nagelberg AS, Worrell WL. Study of sodium-intercalated TaS2 and TiS2. J Solid State Chem 1979;29:345.
[35] Delmas C, Braconnier JJ, Fouassier C, Hagenmuller P. Electrochemical intercalaction of sodium in Na_xCoO_2 bronzes. Solid State Ionics 1981;4:165.
[36] Molenda J, Delmas C, Hagenmuller P. Electronic and electrochemical properties of Na_xCo_{2-y} cathode. Solid State Ionics 1983;10:431.
[37] Shacklette LW, Jow TR, Townsend L. Rechargeable electrodes from sodium cobalt bronzes. J Electrochem Soc 1985;135:2669.
[38] Tarascon JM, Hull GW. Sodium intercalaction into the layered oxides NaxMoO$_4$. Solid State Ionics 1986;22:85.
[39] Jow TR, Shacklette LW, Maxfield M, Vernick D. The role of conductive polymers in alkali-metal secondary electrodes. J Electrochem Soc 1987;134:1730.
[40] West K, Zachau-Christiansen B, Jacobsen T, Skaarup S. Sodium insertion in vanadium oxides. Solid State Ionics 1988;30:1128.
[41] Sauvage F, Laffont L, Tarascon J-M, Baudrin E. Study of the insertion/deinsertion mechanism of sodium into $Na_{0.44}MnO_2$.. Inorg Chem 2007;46:3289.
[42] Cao Y, Xiao L, Wang W, Choi D, Nie Z, Yu J, et al. Reversible sodium ion insertion in single crystalline manganese oxide nanowires with long cycle life. Adv Mater 2011;23:3155.

[43] Doeff MM, Peng MY, Ma Y, De Jonghe LC. Orthorhombic Na_xMnO_2 as a cathode material for secondary sodium and lithium polymer batteries. J Electrochem Soc 1994;141:L145.

[44] Zhang C, Gamble S, Ainsworth D, Slawin AMZ, Andreev YG, Bruce PG. Alkali metal crystalline polymer electrolytes. Nat Mater 2009;8:580.

[45] Tevar AD, Whitacre JF. Relating synthesis conditions and electrochemical performance for the sodium intercalation compound Na[sub 4]Mn[sub 9]O[sub 18] in aqueous electrolyte. J Electrochem Soc 2010;157:A870.

[46] Tarascon JM, Guyomard DG, Wilkens B, Kinnon WRM, Barboux P. Chemical and electrochemical insertion of Na into the spinel MnO_2 phase. Solid State Ionics 1992;57:113.

[47] Ohzuku T, Ueda A, Nagayama M, Iwakoshi Y, Komori H. Comparative study of LiCoO2, $LiNiCoO_2$ and $LiNiO_2$ for 4 volt secondary lithium cells. Electrochim Acta 1993;38:1159.

[48] Ozawa K. Lithium-ion rechargeable batteries with $LiCoO_2$ and carbon electrodes: the $LiCoO_2$/C system. Solid State Ionics 1994;69:212.

[49] Yazami R, Lebrun N, Bonneau M, Molteni M. High performance $LiCoO_2$ positive electrode material. J Power Sources 1995;54:389.

[50] Ohzuku T, Makimura Y. Layered lithium insertion material of LiNi1/2Mn1/$2O_2$: a possible alternative to $LiCoO_2$ for advanced lithium-ion batteries. Chem Lett 2001;2:744.

[51] Berthelot R, Carlier D, Delmas C. Electrochemical investigation of the P2–Na_xCoO_2 phase diagram. Nat Mater 2011;10:74.

[52] Ma X, Chen H, Ceder G. Electrochemical properties of monoclinic NaMnO2. J Electrochem Soc 2011;158:A1307.

[53] Parant J-P, Olazcuaga R, Devalette M, Fouassier C, Hagenmuller ETP, et al. Sur quelques nouvelles phases de formule Na, MnO, (x G 1). J Solid State Chem 1971;3:1.

[54] Velikokhatnyi OI, Chang C-C, Kumta PN. Phase stability and electronic structure of NaMnO[sub 2]. J Electrochem Soc 2003;150:A1262.

[55] Mendiboure A, Delmas C, Hagenmuller P. Electrochemical intercalation and deintercalation of Na_xMnO_2 bronzes. J Solid State Chem 1985;57:323.

[56] Bhide A, Hariharan K. Physicochemical properties of Na_xCoO_2 as a cathode for solid state sodium battery. Solid State Ionics 2010;192:360.

[57] Carlier D, Cheng JH, Berthelot R, Guignard M, Yoncheva M, Stoyanova R, et al. Physical properties and electrochemical behavior as positive electrode in sodium battery. Dalton Trans 2011;40:9306.

[58] Kim D, Kang S-H, Slater M, Rood S, Vaughey JT, Karan N, et al. Enabling sodium batteries using lithium-substituted sodium layered transition metal oxide cathodes. Adv Energy Mater 2011;1:333.

[59] Ong SP, Chevrier VL, Hautier G, Jain A, Moore C, Kim S, et al. Voltage, stability and diffusion barrier differences between sodium-ion and lithium-ion intercalation materials. Energy Environ Sci 2011;4:3680.

[60] Hasegawa Y, Imanaka N. Effect of the lattice volume on the Al^{3+} ion conduction in NASICON type solid electrolyte. Solid State Ionics 2005;176:2499.

[61] Hoshina K, Dokko K, Kanamura K. Investigation on electrochemical interface between $Li_4Ti_5O_{12}$ and $Li_1 + xAl_xTi_2 - x(PO_4)_3$ NASICON-type solid electrolyte. J Electrochem Soc 2005;152:2138.

[62] Kobayashi E, Plashnitsa LS, Doi T, Okada S, Yamaki J-I. Electrochemistry communications electrochemical properties of Li symmetric solid-state cell with NASICON-type solid electrolyte and electrodes. Electrochem Commun 2010;12:894.

[63] Tillement O, Angenault J, Couturier JC, Quarton M. Electrochemical studies of mixed valence NASICON. Solid State Ionics 1992;56:391.

[64] Patoux S, Rousse G, Leriche J-B, Masquelier C. Structural and electrochemical studies of rhombohedral $Na_2TiM(PO_4)_3$ and $Li1.6Na_{0.4}TiM(PO_4)_3$ (M = Fe, Cr) phosphates. Chem Mater 2003;3:2084.

[65] Pahdi AK, Nanjundaswamy KS, Masquelier C, Okada S, Goodenough JB. Effect of structure on the Fe^{3+}/Fe^{2+} redox couple in iron phosphates. J Electrochem Soc 1997;144:1609.

[66] Uebou Y, Kiyabu T, Okada S, Yamaki J-I. Kyushu University NII-electronic library service. The Rep Inst Adv Mater Study 2002;16:1.

[67] Barker J, Gover RKB, Burns P, Bryan A. A symmetrical lithium-ion cell based on lithium vanadium fluorophosphate, $LiVPO_4F$. Electrochem. Solid-State Lett. 2005;8:A285.

[68] Plashnitsa LS, Kobayashi E, Noguchi Y, Okada S, Yamaki J-I. Performance of NASICON symmetric cell with ionic liquid electrolyte. J Electrochem Soc 2010;157:A536.

[69] Pahdi AK, Nanjundaswamy KS, Goodenough JB. Phospho-olivines as positive-electrode materials for rechargeable lithium batteries. J Electrochem Soc 1997;144:1188.

[70] Ellis BL, Makahnouk WRM, Makimura Y, Toghill K, Nazar LF. A multifunctional 3.5 V iron-based phosphate cathode for rechargeable batteries. Nat Mater 2007;6:749.

[71] Zaghib K, Trottier J, Hovington P, Brochu F, Guerfi A, Mauger A, et al. Characterization of Na-based phosphate as electrode materials for electrochemical cells. J Power Sources 2011;196:9612.

[72] Moreau P, Guyomard D, Gaubicher J, Boucher F. Structure and stability of sodium intercalated phases in olivine $FePO_4$. Chem Mater 2010;22:4126.

[73] Chevrier VL, Ceder G. Challenges for Na-ion negative electrodes. J Electrochem Soc 2011;158:A1011.

[74] Shiratsuchi T, Okada S, Yamaki J, Nishida T. $FePO_4$ cathode properties for Li and Na secondary cells. J Power Sources 2006;159:268.

[75] Lee KT, Ramesh TN, Nan F, Botton G, Nazar LF. Topochemical synthesis of sodium metal phosphate olivines for sodium-ion batteries. Chem Mater 2011;23:3593.

[76] Yamada A, Kudo Y, Liu K-Y. Phase diagram of $Li_x(Mn_{[y]}Fe_{[1-y]})PO_4$ $(0 \leqslant x, y \leqslant 1)$. J Electrochem Soc 2001;148:A1153.

[77] Barker J, Saidi MY, Swoyer JL. A sodium-ion cell based on the fluorophosphate compound $NaVPO_4F$. Electrochem Solid-State Lett 2003;6:A1.

[78] Sauvage F, Quarez E, Tarascon J-M, Baudrin E. Crystal structure and electrochemical properties vs. Na^+ of the sodium fluorophosphate $Na_{1.5}VOPO_4F_{0.5}$. Solid State Sci 2006;8:1215.

[79] Barker J, Gover RKB, Burns P, Bryan AJ. Hybrid-ion a lithium-ion cell based on a sodium insertion material. Electrochem Solid-State Lett 2006;9:A190.

[80] Swafford S, Holt EM. New synthetic approaches to monophosphate fluoride ceramics: synthesis and structural characterization of $Na_2Mg(PO_4)F$ and $Sr_5(PO_4)3F$. Solid State Sci 2002;4:807.

[81] Sanz F, Parada C, Ruíz-Valero C. Crystal growth, crystal structure and magnetic properties of disodium cobalt fluorophosphate. J Mater Chem 2001;11:208.

[82] Recham N, Chotard J-N, Dupont L, Djellab K, Armand M, Tarascon J-M. Ionothermal synthesis of sodium-based fluorophosphate cathode materials. J Electrochem Soc 2009;156:A993.

[83] Ellis BL, Makahnouk WRM, Rowan-Weetaluktuk WN, Ryan DH, Nazar LF. Crystal structure and electrochemical properties of A_2MPO_4F fluorophosphates (A = Na, Li; M = Fe, Mn, Co, Ni). Chem Mater 2010;22:1059.

[84] Tripathi R, Ramesh TN, Ellis BL, Nazar LF. Scalable synthesis of tavorite $LiFeSO_4F$ and $NaFeSO_4F$ cathode materials. Angew Chem Int Ed 2010;49:8738.

[85] Barpanda P, Chotard J-N, Recham N, Delacourt C, Ati M, Dupont L, et al. Structural, transport, and electrochemical investigation of novel AMSO4F (A = Na, Li; M = Fe, Co., Ni, Mn) metal fluorosulphates prepared using low temperature synthesis routes.. Inorg Chem 2010;49:7401.

[86] Pizarro-Sanz J, Dance J, Villeneuve G, Arriortua-Marcaida M. The natural and synthetic tavorite minerals: crystal chemistry and magnetic properties. Mater Lett 1994;18:327.

[87] Tripathi R, Gardiner GR, Islam MS, Nazar LF. Alkali-ion conduction paths in LiFeSO4F and NaFeSO4F tavorite-type cathode materials. Chem Mater 2011;23:2278.

[88] Asher RC. A lamellar compound of sodium and graphite. J Inorg Nucl Chem 1959;10:238.

[89] Ge P, Fouletier M. Electrochemical intercalation of sodium in graphite. Solid State Ionics 1988;30:1172.

[90] Stevens DA, Dahn JR. The mechanisms of lithium and sodium insertion in carbon materials. J Electrochem Soc 2001;148:A803.

[91] Doeff MM, Ma Y, Visco SJ, De Jonghe LC. Electrochemical insertion of sodium into carbon. J Electrochem Soc 1993;140:L169.

[92] Stevens DA, Dahn JR. High capacity anode materials for rechargeable sodium-ion batteries. J Electrochem Soc 2000;147:1271.

[93] Wenzel S, Hara T, Janek J, Adelhelm P. Room-temperature sodium-ion batteries: improving the rate capability of carbon anode materials by templating strategies. Energy Environ Sci 2011;4:3342.

[94] Park SI, Gocheva I, Okada S, Yamaki J-I. Electrochemical properties of $NaTi_2(PO_4)_3$ anode for rechargeable aqueous sodium-ion batteries. J Electrochem Soc 2011;158:A1067.

[95] Xiong H, Slater MD, Balasubramanian M, Johnson CS, Rajh T. Amorphous TiO_2 nanotube anode for rechargeable sodium ion batteries. J Phys Chem Lett 2011;2:2560–5.

[96] Senguttuvan P, Palacín MR. $Na_2Ti_3O_7$: lowest voltage ever reported oxide insertion electrode for sodium ion batteries. Chem Mater 2011;23:4109.

[97] Didier C, Guignard M, Denage C, Szajwaj O, Ito S, Saadoune I, et al. Electrochemical Na-deintercalation from $NaVO_2$. Electrochem Solid-State Lett 2011;14:A75.

[98] Szajwaj O, Gaudin E, Weill F, Darriet J, Delmas C. Investigation of the new P′3-$Na_{0.60}VO_2$ phase: structural and physical properties.. Inorg Chem 2009;48:9147.

[99] Hamani D, Ati M, Tarascon J-M, Rozier P. Na_xVO_2 as possible electrode for Na-ion batteries. Electrochem Commun 2011;13:938.

[100] Liu H, Zhou H, Chen L, Tang Z, Yang W. Electrochemical insertion/deinsertion of sodium on NaV_6O_{15} nanorods as cathode material of rechargeable sodium-based batteries. J Power Sources 2011;196:814.

[101] Yang Z, Zhang J, Kintner-Meyer MCW, Lu X, Choi D, Lemmon JP, et al. Electrochemical energy storage for green grid. Chem Rev 2011;111:3577.